

Manipulation of a Nuclear NAD⁺ Salvage Pathway Delays Aging without Altering Steady-state NAD⁺ Levels*

Received for publication, December 10, 2001, and in revised form, March 4, 2002
Published, JBC Papers in Press, March 7, 2002, DOI 10.1074/jbc.M111773200

Rozalyn M. Anderson^{‡§}, Kevin J. Bitterman^{‡§}, Jason G. Wood^{‡¶}, Oliver Medvedik[‡],
Haim Cohen^{‡||}, Stephen S. Lin^{**}, Jill K. Manchester^{**}, Jeffrey I. Gordon^{**},
and David A. Sinclair^{‡‡}

From the [‡]Department of Pathology, Harvard Medical School, Boston, Massachusetts 02115 and the ^{**}Department of Molecular Biology and Pharmacology, Washington University School of Medicine, St. Louis, Missouri 63110

Yeast deprived of nutrients exhibit a marked life span extension that requires the activity of the NAD⁺-dependent histone deacetylase, Sir2p. Here we show that increased dosage of *NPT1*, encoding a nicotinate phosphoribosyltransferase critical for the NAD⁺ salvage pathway, increases Sir2-dependent silencing, stabilizes the rDNA locus, and extends yeast replicative life span by up to 60%. Both *NPT1* and *SIR2* provide resistance against heat shock, demonstrating that these genes act in a more general manner to promote cell survival. We show that *Npt1* and a previously uncharacterized salvage pathway enzyme, *Nma2*, are both concentrated in the nucleus, indicating that a significant amount of NAD⁺ is regenerated in this organelle. Additional copies of the salvage pathway genes, *PNC1*, *NMA1*, and *NMA2*, increase telomeric and rDNA silencing, implying that multiple steps affect the rate of the pathway. Although *SIR2*-dependent processes are enhanced by additional *NPT1*, steady-state NAD⁺ levels and NAD⁺/NADH ratios remain unaltered. This finding suggests that yeast life span extension may be facilitated by an increase in the availability of NAD⁺ to Sir2, although not through a simple increase in steady-state levels. We propose a model in which increased flux through the NAD⁺ salvage pathway is responsible for the Sir2-dependent extension of life span.

Physiological studies and, more recently, DNA array analysis of gene expression patterns have confirmed that aging is a complex biological process. In contrast, genetic studies in model organisms have demonstrated that relatively minor changes to an organism's environment or genetic makeup can dramatically slow the aging process. For example, the life span of many diverse organisms can be greatly extended simply by limiting caloric intake, in a dietary regime known as caloric restriction (1–3).

How can simple changes have such profound effects on a complex process such as aging? A picture is emerging in which

all eukaryotes possess a surprisingly conserved regulatory system that governs the pace of aging (4, 5). Such a regulatory system may have arisen in evolution to allow organisms to survive in adverse conditions by redirecting resources from growth and reproduction to pathways that provide stress resistance (4, 6).

One model that has proven particularly useful in the identification of regulatory factors of aging is the budding yeast *Saccharomyces cerevisiae*. Replicative life span in *S. cerevisiae* is typically defined as the number of buds or “daughter cells” produced by an individual “mother cell” (7). Mother cells undergo age-dependent changes, including an increase in size, a slowing of the cell cycle, enlargement of the nucleolus, an increase in steady-state NAD⁺ levels, increased gluconeogenesis and energy storage, and sterility resulting from the loss of silencing at telomeres and mating-type loci (8–13). An alternative measure of yeast life span, known as chronological aging, is the length of time a population of non-dividing cells remains viable when deprived of nutrients (14). Increased chronological life span correlates with increased resistance to heat shock and oxidative stress, suggesting that cumulative damage to cellular components is a major cause of this type of aging (14, 15). The extent of overlap between replicative and chronological aging is currently unclear.

One cause of yeast replicative aging has been shown to stem from the instability of the repeated ribosomal DNA (rDNA)¹ locus (16). This instability gives rise to circular forms of rDNA called extrachromosomal rDNA circles that replicate but fail to segregate to daughter cells. Eventually, extrachromosomal rDNA circles accumulate to over 1000 copies, which are thought to kill cells by titrating essential transcription and/or replication factors (16–18). Regimens that reduce rDNA recombination such as caloric restriction or a *fov1* deletion extend replicative life span (17, 19, 20).

A key regulator of aging in yeast is the Sir2 silencing protein (17), a nicotinamide adenine dinucleotide (NAD⁺)-dependent deacetylase (21–24). Sir2 is a component of the heterotrimeric Sir2/3/4 complex that catalyzes the formation of silent heterochromatin at telomeres and the two silent mating-type loci (25). Sir2 is also a component of the regulator of nucleolar silencing and telophase exit complex that is required for silencing at the rDNA locus and exit from telophase (26, 27). This complex has also recently been shown to directly stimulate transcription of

* Work was supported in part by The Ellison Foundation, The American Federation for Aging Research, and The Arminese Foundation. The costs of publication of this article were defrayed in part by the payment of page charges. This article must therefore be hereby marked “advertisement” in accordance with 18 U.S.C. Section 1734 solely to indicate this fact.

§ Both authors contributed equally to this work.

|| Supported by a Taplan Fellowship.

¶ Supported by a National Science Foundation scholarship.

‡‡ Supported by a Leukemia and Lymphoma Society Special Fellowship. To whom correspondence should be addressed: Dept. of Pathology, Harvard Medical School, 200 Longwood Ave., Boston, MA 02115. Tel.: 617-432-3931; Fax: 617-432-1313; E-mail: david_sinclair@hms.harvard.edu.

¹ The abbreviations used are: rDNA, ribosomal DNA; NaMN, nicotinic acid mononucleotide; NaAD, desamido-NAD⁺; NaM, nicotinamide; NaMNAT, nicotinate mononucleotide adenyltransferase; ORF, open reading frame; GFP, green fluorescence protein; HA, hemagglutinin; SC, synthetic complete; MMS, methylmethane sulfonate; 3xHA, triple hemagglutinin epitope.

rRNA by polymerase I and to be involved in the regulation of nucleolar structure (28).

Biochemical studies have shown that Sir2 can readily deacetylate the amino-terminal tails of histones H3 and H4, resulting in the formation of *O*-acetyl-ADP-ribose and nicotinamide (21–23, 29). Strains with additional copies of *SIR2* display increased rDNA silencing (30) and a 30% longer life span (17). It has recently been shown that additional copies of the *Caenorhabditis elegans* *SIR2* homolog, *sir-2.1*, greatly extend life span in that organism (31). This implies that the *SIR2*-dependent regulatory pathway for aging arose early in evolution and has been well conserved (4). Yeast life span, like that of metazoans, is also extended by interventions that resemble caloric restriction (19, 32). Mutations that reduce the activity of the glucose-responsive cAMP (adenosine 3',5'-monophosphate)-dependent (protein kinase A) pathway extend life span in wild type cells but not in mutant *sir2* strains, demonstrating that *SIR2* is a key downstream component of the caloric restriction pathway (19).

In bacteria, NAD⁺ is synthesized *de novo* from tryptophan and recycled in four steps from nicotinamide via the NAD⁺ salvage pathway (see Fig. 5 below). The first step in the bacterial NAD⁺ salvage pathway, the hydrolysis of nicotinamide to nicotinic acid and ammonia, is catalyzed by the *pncA* gene product (33). An *S. cerevisiae* gene with homology to *pncA*, *YGL037*, was recently assigned the name *PNC1* (34). A nicotinate phosphoribosyltransferase, encoded by the *NPT1* gene in *S. cerevisiae*, converts the nicotinic acid from this reaction to nicotinic acid mononucleotide (NaMN) (35–38). At this point, the NAD⁺ salvage pathway and the *de novo* NAD⁺ pathway converge and NaMN is converted to desamido-NAD⁺ (NaAD) by a nicotinate mononucleotide adenyltransferase (NaMAT). In *S. cerevisiae*, there are two putative ORFs with homology to bacterial NaMNAT genes, *YLR328* (39) and an uncharacterized ORF, *YGR010* (23, 39). We refer to these two ORFs as *NMA1* and *NMA2*, respectively. In *Salmonella*, the final step in the regeneration of NAD⁺ is catalyzed by an NAD synthetase (40). An as yet uncharacterized ORF, *QNS1*, is predicted to encode an NAD synthetase (23).

In yeast, null mutations in *NPT1* reduce steady-state NAD⁺ levels by ~2-fold (23) and abolish the longevity provided by limiting calories (19). One current hypothesis explaining how caloric restriction extends replicative life span is that decreased metabolic activity causes an increase in NAD⁺ levels, which then stimulate Sir2 activity (reviewed in Campisi (68) and Guarente (69)). In this study, we tested this theory by examining whether additional copies of *NPT1* can promote Sir2-dependent life span extension and whether this correlates with increased NAD⁺ levels. We show that additional *NPT1* extends replicative life span in a *SIR2*-dependent manner via the caloric restriction pathway. We find that these long-lived strains do not have increased NAD⁺ levels or altered NAD⁺/NADH ratios, despite the fact that every *SIR2*-dependent process we examined was enhanced. Interestingly, increased dosage of *SIR2* or *NPT1* provides resistance to heat shock, indicating that these genes act in a general manner to promote cell survival.

We find that additional copies of all the salvage pathway genes increase rDNA and telomeric silencing with exception of *QNS1*. We show that *Npt1* and *Nma2* are concentrated in the nucleus, raising the possibility that a substantial fraction of NAD⁺ is recycled within this organelle. We discuss the potential for extending life span in higher organisms by stimulation of the conserved NAD⁺ salvage pathway.

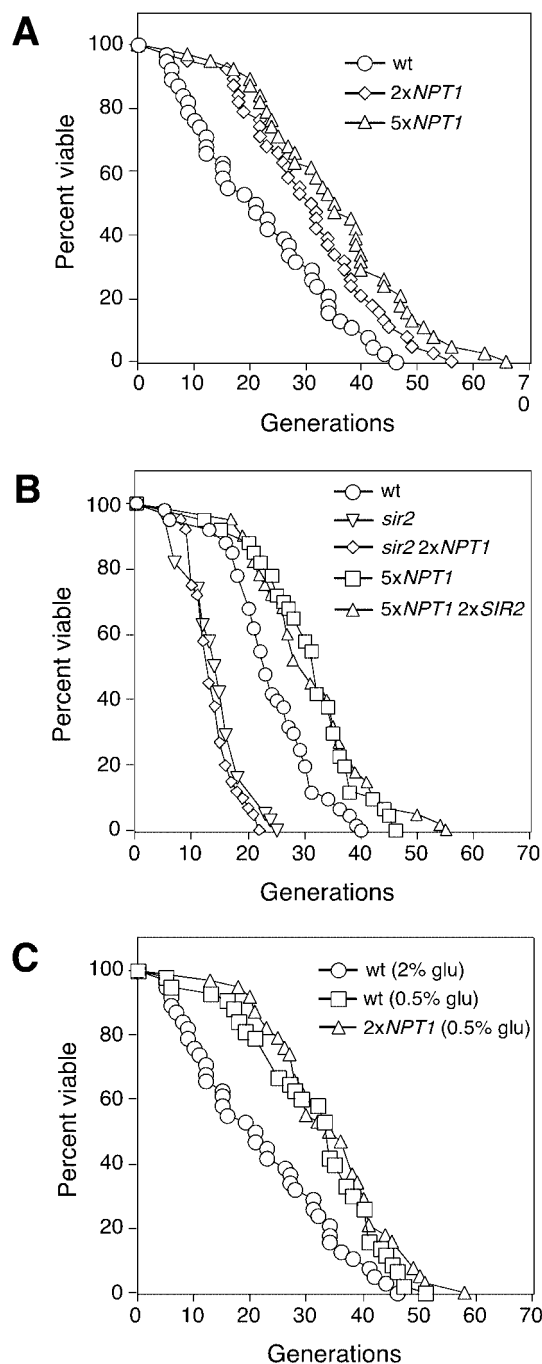


FIG. 1. Increased dosage of *NPT1* delays aging by mimicking caloric restriction. Life span was determined by scoring the number of daughter cells produced by each mother cell before cessation of cell division (7, 10). Cells were pre-grown for a minimum of 48 h on complete glucose medium. **A**, mortality curves for wild type (PSY316AT, circles), *2xNPT1* (YDS1544, diamonds), and *5xNPT1* (YDS1548, triangles) on medium with 2% glucose. Average life spans are 21.9, 30.8, and 35.1 generations, respectively. **B**, mortality curves for wild type (PSY316AT, circles), *sir2::TRP1* (YDS1594, downward triangles), *2xNPT1* (YDS1544, squares), *sir2::TRP1 2xNPT1* (YDS1573, diamonds), and *5xNPT1 2xSIR2* (YDS1577, upward triangles) on 2% glucose medium. Average life spans were 23.7, 14.4, 13.9, 31.0, and 31.9 generations, respectively. **C**, mortality curves for wild type on 2% glucose (PSY316AT, circles) and 0.5% glucose medium (PSY316AT, squares) and for *2xNPT1* on 0.5% glucose medium (YDS1544, triangles). Average life spans are 21.9, 31.7, and 34.5 generations, respectively.

EXPERIMENTAL PROCEDURES

Plasmids and Strains—Strains used in this study are listed in Table II (see below). W303AR5 *sir3::URA3* (16), W303AR5 *sir4::HIS3*,

TABLE I
Steady-state NAD⁺ and NADH levels in various long- and short-lived strains

Genotype	NAD ⁺	NADH	NAD ⁺ /NADH, ratio	ATP
	amol/pg protein ^a		amol/pg protein ^a	
1x <i>NPT1</i> (wild type)	23.7 (3.2)	9.3 (0.8)	2.8 (0.5)	15.5 (3)
2x <i>NPT1</i>	21.9 (2.0)	6.0 (0.6)	3.3 (0.3)	7.6 (1.6)
2x <i>NPT1 sir2::TRP1</i>	22.5 (1.6)	7.0 (0.3)	2.4 (0.9)	5.3 (1.1)
<i>sir2::TRP1</i>	23.6 (1.2)	7.0 (0.6)	2.8 (1.2)	7.9 (1.9)

^a Average of five independent experiments (S.E.).

W303AR5 *sir2::TRP1*, and PSY316AT have been described previously (41). Deletion of *SIR2* in PSY316AT was performed using *ScaI/PvuII*-linearized pC369 (41). JS209, JS241, JS237, and JS218 were gifts from J. Smith (42). The coding region and 1.1 kb of upstream sequence of *NPT1* were amplified by PCR (43), and the 2.4-kb product fragment was subcloned into the pRS306 based vector pSP400 between *NotI* and *SacI* (gift from L. Guarente, M.I.T.) and the 2 μ -based vector pDB20 (44) to generate pSPNPT1 and pDBNPT1, respectively.

Additional copies of *NPT1* were integrated at the *URA3* locus using plasmid pSPNPT1 linearized with *StuI*. Integrants were first identified by PCR. The *NPT1* copy-number was then determined by probing for *NPT1* and *ACT1* DNA on Southern blots. The density of the *NPT1* band was compared with an *ACT1* band using ImageQuant software (Molecular Dynamics, Sunnyvale, CA). Strains carrying an additional copy of *SIR2* were generated by integrating plasmids p306SIR2 or p305SIR2 (17) linearized with *XcmI*. High copy *SIR2* was introduced on the 2 μ -based plasmid p2 μ SIR2 (gift of L. Pillus, University of California at San Diego). W303AR5 was transformed to Ura⁺ and Leu⁺ prototrophy by integrating pRS306 or pRS305 (45) linearized with *StuI* and *XcmI*, respectively. YDS1595 was generated from W303AR5 by selecting a colony that had experienced an *ADE2* loss event. YDS1595 was transformed with *StuI*-cut pRS402 (carrying the *ADE2* gene) to create YDS1596. W303cdc25-10 was a gift from S. Lin (M. I. T.) (19). The *NPT1* deletion strain, YDS1580, was generated by replacing the wild type gene with the *kan'* marker as described previously (46). The coding region and 650 bp upstream of *PNC1/YGL037* was amplified by PCR from genomic DNA. The 1350-bp *SacI/NotI* fragment was cloned into the vector pSR400 to generate pSPYGL037. The coding region and 500 bp upstream of *NMA2/YGR010* were amplified by PCR from genomic template, and the 1730-bp *SacI/NotI* fragment was cloned into pSP400 to generate pSPYGR010. The coding region of *NMA1/YLR328* and 450 bp upstream were amplified from genomic template by PCR, and the 2150-bp fragment was cloned into pRS306 to generate p306YLR328. The coding region and 600 bp upstream of *QNS1/YHR074* were amplified by PCR, and the 2.8-kb *SacI/NotI* fragment was cloned into pSP400 to make pSPYHR074. Additional copies of *PNC1/YGL037*, *NMA1/YLR328*, *NMA2/YGR010*, and *QNS1/YHR074* were integrated at the *URA3* locus of W303AR5 and PSY316AT by transformation. All amplified DNA was confirmed to be free of mutations by sequencing.

HA-tagged *NPT1* was generated using a tag-*kan'* integration method (47) in strains W303AR5 and W303cdc25-10 (19). A green fluorescence protein (GFP) cassette was introduced at the carboxyl terminus of Npt1, Nma1, and Nma2 as described previously (48). The functionality of tagged proteins was confirmed by assaying rDNA silencing.

Life Span Determination—Replicative life span determination was performed as described (16). Cells were grown on YPD medium (1% yeast extract, 2% bacto-peptone, 2% glucose w/v) unless otherwise stated with a minimum of 40 cells per experiment. Each experiment was performed at least twice independently. Statistical significance of life span differences was determined using the Wilcoxon rank sum test. Differences are stated to be different when the confidence is higher than 95%.

mRNA and Protein Determination—Northern and Western blots were performed using standard techniques. *NPT1* transcripts were detected using a probe derived from the complete open reading frame of the *NPT1* gene. *ACT1* mRNA was detected using a full-length *ACT1* probe (gift of G. Fink, M. I. T.). The HA epitope tag was detected using monoclonal antibody HA.11 (Covance Research Products, Richmond, CA). Actin was detected with monoclonal antibody MAB1501R (Chemicon, Temecula, CA).

Yeast Assays and GFP Localization—Yeast strains were grown at 30 °C unless otherwise stated. The extent of silencing at the ribosomal DNA locus was determined using two assays. For the *ADE2* silencing assay, cells were pre-grown on synthetic complete (SC) medium (1.67% yeast nitrogen base, 2% glucose, 40 mg/liter each of histidine, uridine,

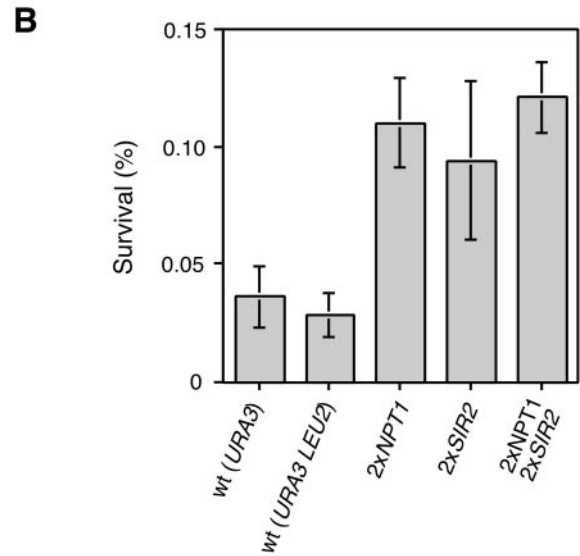
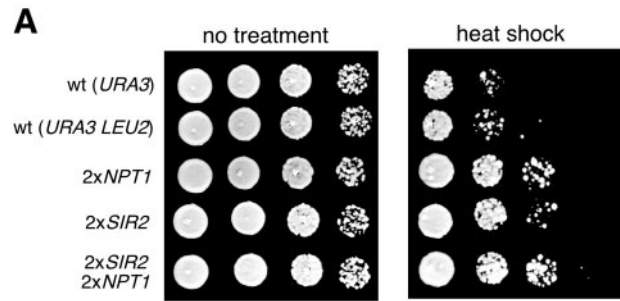


FIG. 2. *NPT1* and *SIR2* provide resistance to heat shock. A, strains were grown for 3 days post-diauxic shift in SC medium and incubated for 1 h at 55 °C before plating 10-fold dilutions on SC plates. B, strains were treated as in A and plated on SC at low density. Colonies that arose after 24 h were scored and expressed as a percentage of colonies arising from the untreated sample. Values represent the average of three independent experiments (\pm S.D.). Strains: W303AR *URA3* (YDS1568), W303AR *URA3 LEU2* (YDS1563), and isogenic derivatives of W303AR, 2x*NPT1-URA3* (YDS1503), 2x*SIR2-URA3* (YDS1572), and 2x*NPT1-URA3 2xSIR2-LEU2* (YDS1561).

tryptophan, adenine, and leucine) for 3 days. Cells were resuspended in SC medium and serially diluted 10-fold in phosphate-buffered saline and spotted onto SC medium lacking adenine. *MET15* silencing assays were performed on Pb²⁺-containing plates as previously described (42). Telomeric silencing was assayed on SC medium containing 0.7 mg/liter adenine. Cells were grown for 3 days and placed at 4 °C for 3 days to enhance color. Heat shock assays were performed essentially as described (14). Strains were pre-grown overnight in SC-complete medium with limiting histidine (20 mg/ml), diluted to 1×10^5 cells/ml in 3 ml of the same medium and grown for 5 days. Cultures were diluted 10-fold in expired medium, incubated for 1 h at 55 °C, and spotted on SC plates. Ribosomal DNA recombination rates were determined as previously described (49). At least 10,000 colonies were examined for each strain and each experiment was performed in triplicate.

NAD⁺ and NADH determinations were measured as described elsewhere (50). Cells expressing a GFP fusion were grown to mid log phase in YPD medium or YPD low glucose (0.5% w/v) then incubated in phosphate-buffered saline containing 20 μ M Hoechst 33342 DNA stain (Sigma Chemical Co.) for 5 min. Images were captured at 100 \times magnification on a Nikon E600 fluorescence microscope and analyzed using Photoshop 6.0 software.

RESULTS

Increased Dosage of *NPT1* Increases Longevity but Not Steady-state NAD⁺ Levels—*SIR2* is a limiting component of longevity in yeast and requires NAD⁺ for catalysis. Studies in *Escherichia coli* have shown that PncB catalyzes a rate-limiting step in the salvage pathway that recycles NAD⁺ (35, 37,

TABLE II
Yeast strains used in this study

Strain	Genotype
W303AR5	W303 MATa, <i>ade2-1, leu2-3,112, can1-100, trp1-1, ura3-52, his3-11,15, RDN1::ADE2, RAD5</i>
YDS878	W303 MATa, <i>ade2-1, leu2-3,112, can1-100, trp1-1, ura3-52, his3-11,15, RDN1::ADE2, RAD5, sir2:TRP1</i>
YDS924	W303AR5 MATa, <i>ade2-1, leu2-3,112, can1-100, trp1-1, ura3-52, his3-11,15, RDN1::ADE2, RAD5, sir3:HIS3</i>
YDS882	W303 MATa, <i>ade2-1, leu2-3,112, can1-100, trp1-1, ura3-52, his3-11,15, RDN1::ADE2, RAD5, sir4:HIS3</i>
YDS1503	W303 MATa, <i>ade2-1, leu2-3,112, can1-100, trp1-1, ura3-52, his3-11,15, RDN1::ADE2, RAD5, URA3/NPT1</i>
YDS1504	W303 MATa, <i>ade2-1, leu2-3,112, can1-100, trp1-1, ura3-52, his3-11,15, RDN1::ADE2, RAD5, sir2:TRP1, URA3/NPT1</i>
YDS1505	W303 MATa, <i>ade2-1, leu2-3,112, can1-100, trp1-1, ura3-52, his3-11,15, RDN1::ADE2, RAD5, sir3:HIS3, URA3/NPT1</i>
YDS1506	W303 MATa, <i>ade2-1, leu2-3,112, can1-100, trp1-1, ura3-52, his3-11,15, RDN1::ADE2, RAD5, sir4:HIS3, URA3/NPT1</i>
YDS1496	W303 MATa, <i>ade2-1, leu2-3,112, can1-100, trp1-1, ura3-52, his3-11,15, RDN1::ADE2, RAD5, pDBNPT1</i>
YDS1494	W303 MATa, <i>ade2-1, leu2-3,112, can1-100, trp1-1, ura3-52, his3-11,15, RDN1::ADE2, RAD5, sir2:TRP1, pDBNPT1</i>
YDS1587	W303 MATa, <i>ade2-1, leu2-3,112, can1-100, trp1-1, ura3-52, his3-11,15, RDN1::ADE2, RAD5, sir3:HIS3, pDBNPT1</i>
YDS1495	W303 MATa, <i>ade2-1, leu2-3,112, can1-100, trp1-1, ura3-52, his3-11,15, RDN1::ADE2, RAD5, sir4:HIS3, pDBNPT1</i>
YDS1572	W303 MATa, <i>ade2-1, leu2-3,112, can1-100, trp1-1, ura3-52, his3-11,15, RDN1::ADE2, RAD5, LEU2/SIR2</i>
YDS1561	W303 MATa, <i>ade2-1, leu2-3,112, can1-100, trp1-1, ura3-52, his3-11,15, RDN1::ADE2, RAD5, URA3/NPT1, LEU2/SIR2</i>
YDS1595	W303 MATa, <i>ade2-1, leu2-3,112, can1-100, trp1-1, ura3-52, his3-11,15, RAD5</i>
YDS1596	W303 MATa, <i>ADE2, leu2-3,112, can1-100, trp1-1, ura3-52, his3-11,15, RAD5</i>
YDS1568	W303 MATa, <i>ade2-1, leu2-3,112, can1-100, trp1-1, URA3, his3-11,15, RDN1::ADE2, RAD5</i>
YDS1563	W303 MATa, <i>ade2-1, LEU2, can1-100, trp1-1, URA3, his3-11,15, RDN1::ADE2, RAD5</i>
YDS1588	W303 MATa, <i>ade2-1, leu2-3,112, can1-100, trp1-1, ura3-52, his3-11,15, RDN1::ADE2, RAD5, pSPYGL037</i>
YDS1589	W303 MATa, <i>ade2-1, leu2-3,112, can1-100, trp1-1, ura3-52, his3-11,15, RDN1::ADE2, RAD5, pSPYGR010</i>
YDS1590	W303 MATa, <i>ade2-1, leu2-3,112, can1-100, trp1-1, ura3-52, his3-11,15, RDN1::ADE2, RAD5, p306YLR328</i>
YDS1614	W303 MATa, <i>ade2-1, leu2-3,112, can1-100, trp1-1, ura3-52, his3-11,15, RDN1::ADE2, RAD5, p306YHR074</i>
YDS1531	W303 MATa, <i>ade2-1, leu2-3,112, can1-100, trp1-1, ura3-52, his3-11,15, RDN1::ADE2, RAD5, NPT1-HA</i>
W303cdc25-10	W303 MATa, <i>ade2-1, leu2-3,112, can1-100, trp1-1, ura3-52, his3-11,15, RDN1::ADE2, RAD5, cdc25-10</i>
YDS1537	W303 MATa, <i>ade2-1, leu2-3,112, can1-100, trp1-1, ura3-52, his3-11,15, RDN1::ADE2, RAD5, cdc25-10, NPT1-HA</i>
YDS1611	W303 MATa, <i>ade2-1, leu2-3,112, can1-100, trp1-1, ura3-52, his3-11,15, RDN1::ADE2, RAD5, NPT1-GFP</i>
YDS1625	W303 MATa, <i>ade2-1, leu2-3,112, can1-100, trp1-1, ura3-52, his3-11,15, RDN1::ADE2, RAD5, NMA1-GFP</i>
YDS1624	W303 MATa, <i>ade2-1, leu2-3,112, can1-100, trp1-1, ura3-52, his3-11,15, RDN1::ADE2, RAD5, NMA2-GFP</i>
PSY316AT	MATα, <i>ura3-53 leu2-3,112 his3-Δ200 ade2-1,01 can1-100 ADE2-TEL V-R</i>
YDS1594	PSY316 MATα, <i>ura3-53 leu2-3,112 his3-Δ200 ade2-1,01 can1-100 ADE2-TEL V-R, sir2:TRP1</i>
YDS1544	PSY316 MATα, <i>ura3-53 leu2-3,112 his3-Δ200 ade2-1,01 can1-100 ADE2-TEL V-R, URA3/NPT1</i>
YDS1548	PSY316 MATα, <i>ura3-53 leu2-3,112 his3-Δ200 ade2-1,01 can1-100 ADE2-TEL V-R, (4x)URA3/NPT1</i>
YDS1527	PSY316 MATα, <i>ura3-53 leu2-3,112 his3-Δ200 ade2-1,01 can1-100 ADE2-TEL V-R, pDBNPT1</i>
YDS1577	PSY316 MATα, <i>ura3-53 leu2-3,112 his3-Δ200 ade2-1,01 can1-100 ADE2-TEL V-R, (4x)URA3/NPT1, LEU2/SIR2</i>
YDS1573	PSY316 MATα, <i>ura3-53 leu2-3,112 his3-Δ200 ade2-1,01 can1-100 ADE2-TEL V-R, sir2::HIS3, URA3/NPT1</i>
YDS1591	PSY316 MATα, <i>ura3-53 leu2-3,112 his3-Δ200 ade2-1,01 can1-100 ADE2-TEL V-R, pSPYGL037</i>
YDS1592	PSY316 MATα, <i>ura3-53 leu2-3,112 his3-Δ200 ade2-1,01 can1-100 ADE2-TEL V-R, pSPYGR010</i>
YDS1593	PSY316 MATα, <i>ura3-53 leu2-3,112 his3-Δ200 ade2-1,01 can1-100 ADE2-TEL V-R, p306YLR328</i>
JS209	MATα, <i>his3Δ200, leu2Δ1, met15Δ200, trp1Δ63, ura3-167</i>
JS241	JS209 MATα, <i>his3Δ200, leu2Δ1, met15Δ200, trp1Δ63, ura3-167, MET15</i>
JS237	JS209 MATα, <i>his3Δ200, leu2Δ1, met15Δ200, trp1Δ63, ura3-167, RDN1::Ty-MET15</i>
JS218	JS237 MATα, <i>his3Δ200, leu2Δ1, met15Δ200, trp1Δ63, ura3-167, RDN1::Ty-MET15, sir2::HIS3</i>
YDS1583	JS237 MATα, <i>his3Δ200, leu2Δ1, met15Δ200, trp1Δ63, ura3-167, RDN1::Ty-MET15, LEU2/SIR2</i>
YDS1522	JS237 MATα, <i>his3Δ200, leu2Δ1, met15Δ200, trp1Δ63, ura3-167, RDN1::Ty-MET15, p2μSIR2</i>
YDS1580	JS237 MATα, <i>his3Δ200, leu2Δ1, met15Δ200, trp1Δ63, ura3-167, RDN1::Ty-MET15, npt1Δ::kan^r</i>
YDS1581	JS237 MATα, <i>his3Δ200, leu2Δ1, met15Δ200, trp1Δ63, ura3-167, RDN1::Ty-MET1, URA3/NPT1</i>
YDS1493	JS237 MATα, <i>his3Δ200, leu2Δ1, met15Δ200, trp1Δ63, ura3-167, RDN1::Ty-MET15, pDBNPT1</i>

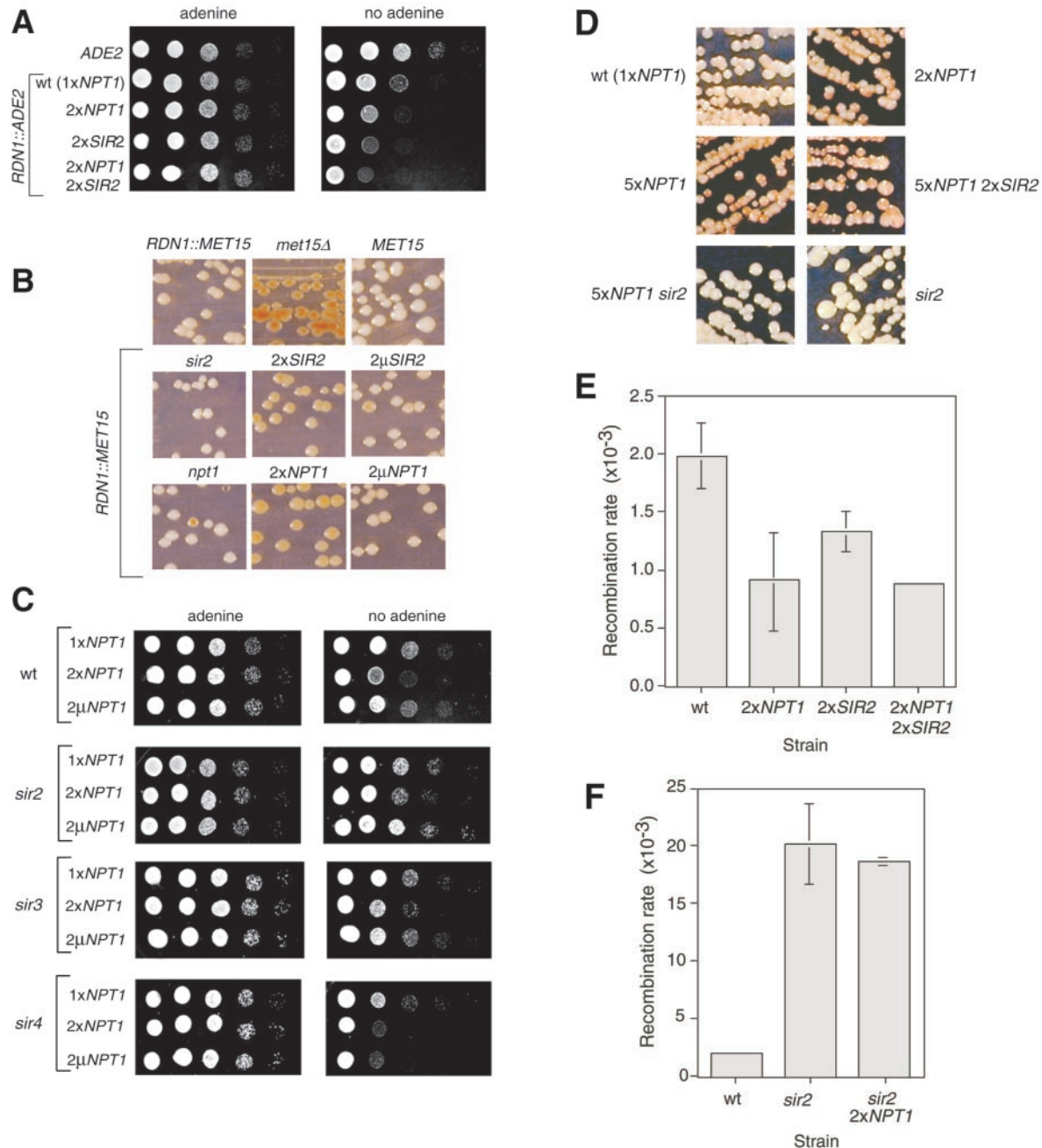


FIG. 3. Additional *NPT1* increases silencing and rDNA stability. A, strains with an *ADE2* marker at the rDNA were pre-grown on SC plates and spotted as 10-fold serial dilutions on SC plates. Increased silencing is indicated by growth retardation on media lacking adenine. Strains: W303-1A *ADE2* (YDS1596), W303-1A *RDN1::ADE2* (W303AR5), and W303AR5 derivatives 2xNPT1 (YDS1503), 2xSIR2 (YDS1572), and 2xNPT1 2xSIR2 (YDS1561). B, silencing of *MET15* at the rDNA locus was assayed by streaking isogenic derivatives of JS237 on rich medium containing 0.07% PbNO₃ and incubating for 5 days at 30 °C. Increased silencing is indicated by accumulation of a brown pigment. Relevant genotypes: *met15Δ* (JS209), *MET15* (JS241), *RND1::MET15* (JS237), *sir2::TRP1* (JS218), 2xSIR2 (YDS1583), 2μSIR2 (YDS1522), *npt1Δ::kan^r* (YDS1580), 2xNPT1 (YDS1581), and 2μNPT1 (YDS1493). C, silencing of an *ADE2* marker at the rDNA locus was determined in strains with 1xNPT1, 2xNPT1, and 2μNPT1 in the following backgrounds: wild type (W303AR5, YDS1503, YDS1496), *sir2::TRP1* (YDS878, YDS1504, YDS1494), *sir3::HIS3* (YDS924, YDS1505, YDS1587), and *sir4::HIS3* (YDS882, YDS1506, YDS1495). D, strains with an *ADE2* marker at the telomere were streaked onto SC medium containing limiting amounts of adenine. Increased silencing is indicated by accumulation of red pigment. Relevant genotypes: (PSY316AT), 2xNPT1 (YDS1544), 5xNPT1 (YDS1548), 5xNPT1 2xSIR2 (YDS1577), and 5xNPT1 *SIR2::TRP1* (YDS1573). *sir2::TRP1* (YDS1594). E, strains in A were assayed for rDNA stability by examining the rate of loss of an *ADE2* marker integrated at the rDNA locus. Cells were plated on YPD medium and the frequency of half-sector colonies, reflecting a marker loss event at the first cell division, was measured. More than 10,000 colonies were examined for each strain and each experiment was performed in triplicate. Average recombination frequencies (± S.D.) per cell division are shown. F, ribosomal DNA recombination rates for wild type (W303AR), *sir2::TRP1* (YDS878), and 2xNPT1 *sir2::TRP1* (YDS1504) strains. Assays were performed as in E.

38). We asked whether additional copies of the yeast *pnkB* homolog, *NPT1*, could increase NAD⁺ production to Sir2 and hence extend yeast life span. *NPT1* was integrated at the *URA3* locus under the control of its native promoter. Strains that carried one or four tandem copies of *NPT1* were then

identified by Southern blotting. We refer to the resulting genotypes as 2xNPT1 and 5xNPT1, respectively.

For the replicative life span assay, cells were grown for at least 2 days on fresh yeast extract/peptone/glucose (YPD) medium to ensure that they had fully recovered from conditions of

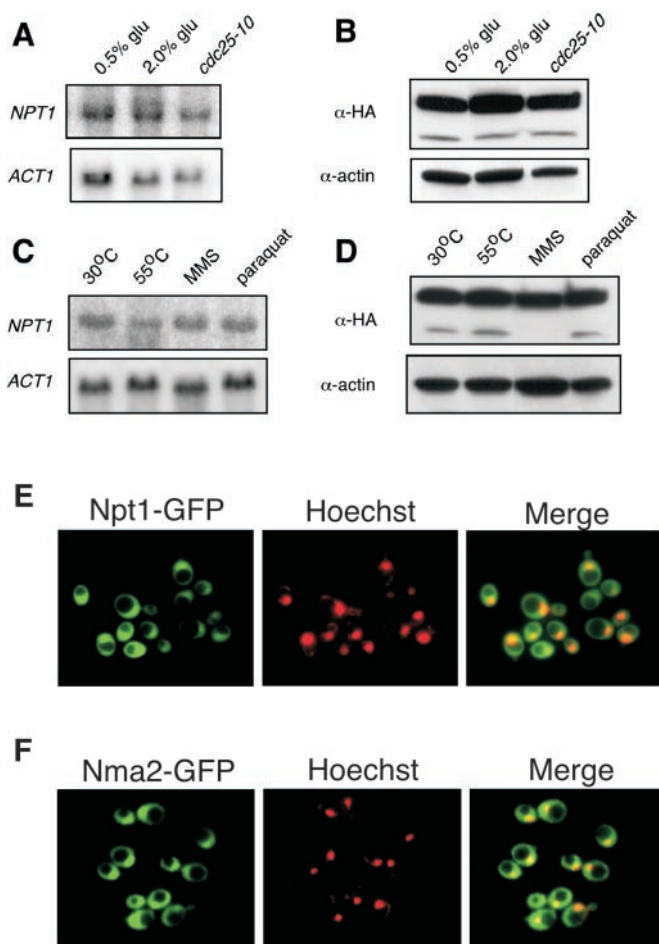


FIG. 4. Analysis of expression and localization of salvage pathway components. A, 3xHA tag sequence was inserted in-frame with the 3'-end of the native *NPT1* ORF in W303AR5 (YDS1531) and W303cdc10–25 (YDS1537). Cells were grown in YPD medium at 30 °C and treated as described. Levels of *NPT1* mRNA were examined for W303AR5 grown in YPD (0.5 and 2.0% glucose) and W303cdc25-10 grown in YPD (2% glucose). A 1.8-kb *NPT1* transcript was detected and levels were normalized to actin (*ACT1*) control. Similar results were obtained in the PSY316 strain background (not shown). B, protein extracts from cultures in A were analyzed by Western blot to detect the HA-tagged Npt1 using α -HA antibody. Two bands of 53 and 40 kDa were detected in the Npt1-HA strain, and no bands were detected in the untagged control strain (not shown). Actin levels served as a loading control. Similar results were obtained in the PSY316 strain background (not shown). C, levels of *NPT1* mRNA were examined in wild type W303AR5 (YDS1531) log phase cultures after 1-h exposure to the following: MMS (0.02% v/v), paraquat (5 mM), or heat shock (55 °C). D, protein extracts of cultures in C were analyzed as in B. In E and F, a green fluorescence protein (GFP) sequence was inserted in-frame at the 3'-end of the native *NPT1* and *NMA2* ORFs in W303AR5 (YDS1611 and YDS1624, respectively). Cells were grown in YPD medium at 30 °C to mid log phase and photographed live. Regions of overlap between GFP (green) and Hoechst DNA stain (red) appear yellow in the merged image.

caloric restriction prior to the assay. Daughter cells that emerged from previously non-budded mother cells were then micro-manipulated away and scored. As shown in Fig. 1A, the 2x*NPT1* strain lived an average of ~40% longer than the wild type strain and the 5x*NPT1* strain lived a striking ~60% longer. The *NPT1*-induced life span extension was completely abrogated by a *sir2* deletion and not significantly enhanced by an additional copy of *SIR2* (Fig. 1B) indicating that the life span extension provided by *NPT1* is mediated by Sir2.

It has recently been shown that wild type cells grown in low glucose medium (0.5% w/v) have an average life span significantly greater than those grown on standard (2%) glucose

medium (19, 32). As shown in Fig. 1C, on low glucose medium the life span of the 5x*NPT1* strain was not significantly greater than the wild type strain. The fact that the effect of *NPT1* and low glucose were not additive suggests that these two regimens act via the same pathway.

Biochemical studies have shown that Sir2 requires NAD⁺ as a cofactor. This has led to the hypothesis that replicative life span may be extended by increased NAD⁺ levels. Consistent with this idea, NAD⁺ levels have been shown to increase significantly in old cells, perhaps as a defense against aging or as the result of decreased metabolic activity (50). To date, the intracellular levels of NAD⁺ in any long-lived strain have not been reported. We found that steady-state NAD⁺ levels and NAD⁺/NADH ratios in the 2x*NPT1* strain were not significantly different from the wild type (Table I). We also examined *sir2* and 2x*NPT1 sir2* strains and again found no difference from wild type, indicating that the failure to detect increased NAD⁺ levels was not due to the activity of Sir2.

NPT1 and SIR2 Increase Resistance to Heat Shock but Not to Other Stresses—Mutations in components of the *C. elegans* and *Drosophila* insulin/insulin-like growth factor-1 pathway allow animals to live up to twice as long as controls (5). In *C. elegans* this longevity is coupled to stress resistance (4). In contrast, the *chico* mutation in *Drosophila*, which extends life span by ~50% in homozygotes, does not appear to protect against heat shock or oxidative stress (51). The link between *sir2.1* life span extension and stress resistance in *C. elegans* has not been examined, although there is evidence from yeast that the Sir2/3/4 complex may be involved in such a response. The yeast *sir4-42* mutation increases replicative life span as well as resistance to starvation and heat shock (52), which raises the possibility that the *SIR2* longevity pathway may also influence stress resistance.

To explore this, we examined the ability of extra copies of *NPT1* and *SIR2* to confer resistance to a variety of stresses, including heat shock, starvation, and exposure to methylmethane sulfonate (MMS) or paraquat. MMS is a DNA-damaging agent that causes a variety of DNA lesions, whereas paraquat induces oxidative stress by generating reactive oxygen species. Additional copies of either *NPT1*, *SIR2*, or both did not provide resistance against paraquat or MMS, nor did they enhance the ability to survive in stationary phase (data not shown).

To assay heat-shock resistance, strains with an additional copy of *NPT1* or *SIR2* were grown to stationary phase in SC medium, heat-shocked for 1 h at 55 °C, then spotted in 10-fold serial dilutions onto SC plates. As shown in Fig. 2A, strains with a single additional copy of *NPT1* or *SIR2* were significantly more resistant to heat shock than the otherwise isogenic wild type control strain. No additive effect of *NPT1* and *SIR2* was apparent, consistent with these two genes acting in the same pathway. To provide a more quantitative measure of this phenotype, strains were subjected to 1 h heat shock and plated for single colonies, and the number of colonies after 24 h was scored as a percentage of the untreated sample. As shown in Fig. 2B, additional copies of *NPT1* and *SIR2*, or both, provided ~3-fold greater survival than wild type, consistent with our earlier finding.

Additional NPT1 Increases Silencing and rDNA Stability—We wished to determine the molecular basis of the *SIR2*-dependent life span extension provided by additional *NPT1*. A simple model predicts that increased dosage of *NPT1* would stimulate the NAD⁺ salvage pathway, which would in turn increase Sir2 activity. We thus examined the effect of additional copies of *NPT1* on the *SIR2*-dependent processes of silencing and stability at the rDNA locus.

To determine the effect of *NPT1* on rDNA silencing, we

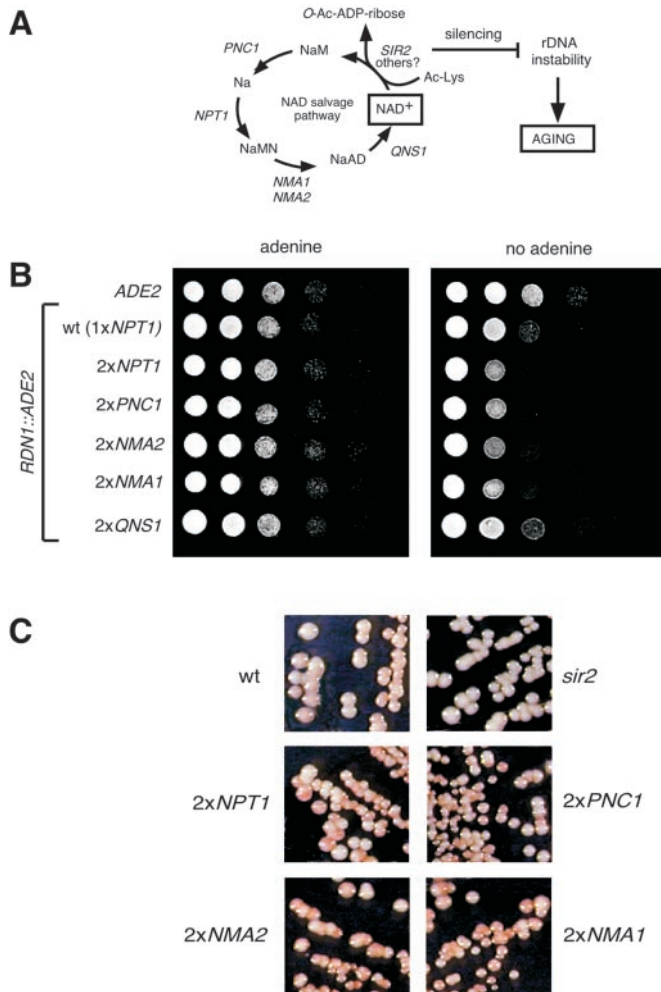


FIG. 5. Multiple limiting components in the NAD⁺ salvage pathway. *A*, the putative steps in NAD⁺ biosynthesis in *S. cerevisiae* based on the known steps in *Salmonella*. The yeast genes that are thought to mediate each step are shown in *italics*. *NaMN*, nicotinic acid mononucleotide; *NaAD*, desamido-NAD⁺; *NaM*, nicotinamide; *Na*, nicotinic acid. Adapted from Smith *et al.* (23). *B*, silencing of *ADE2* at the rDNA locus in strains *ADE2* (YDS1596), wild type (W303AR5), 2x*NPT1* (YDS1503), 2x*PNC1* (YDS1588), 2x*NMA2* (YDS1589), 2x*NMA1* (YDS1590), and 2x*QNS1* (YDS1614). Increased silencing is indicated by growth retardation on media lacking adenine. *C*, strains with an *ADE2* marker at the telomere were streaked onto SC medium containing limiting amounts of adenine. Silencing is indicated by the accumulation of a red pigment. Strains tested: wild type (PSY316AT), 2x*NPT1* (YDS1544), 5x*NPT1* (YDS1548), *sir2::TRP1* (YDS1594), 2x*PNC1* (YDS1591), 2x*NMA2* (YDS1592), and 2x*NMA1* (YDS1593).

utilized strains with either an *ADE2* or *MET15* marker integrated at the rDNA locus (*RDN1*) (Table II). We used two marker genes to ensure that the effects we observed were not simply due to changes in adenine or methionine biosynthesis. Silencing of *ADE2* results in slower growth of cells on media lacking adenine and the accumulation of a red pigment on plates with limiting adenine. Silencing of *MET15* leads to production of a brown pigment on Pb²⁺-containing medium. Strains with additional copies of *SIR2* were included for comparison. The 2x*NPT1* strains showed higher levels of rDNA silencing than wild type in the *ADE2* assay (Fig. 3A, compare growth on adenine with growth on no adenine) and the *MET15* assay (Fig. 3B). Introduction of an additional copy of *NPT1* into the 2x*SIR2* strain did not further increase silencing, again consistent with the placement of these two genes in the same pathway. Strains carrying *SIR2* and *NPT1* on high copy 2 μ -based plasmids also showed increased levels of rDNA silencing,

although not as great as strains carrying single extra copies, for reasons that remain unclear (Fig. 3, B and C). An additional copy of *NPT1* also increased silencing in *sir3* and *sir4* null strains (Fig. 3C). High copy *NPT1* had a disruptive effect on rDNA silencing in the *sir3* strain, whereas this effect was not observed in the *sir4* strain. This can be explained by the fact that *sir4* mutants relocalize Sir2 to the rDNA, which may counteract the high levels of Npt1. Additional copies of *NPT1* in a *sir2* mutant caused a slight increase in rDNA silencing that was considerably weaker than *SIR2*-dependent silencing. The basis of this apparent increase is unclear. To determine whether this was a global effect on silencing, we examined silencing at a telomeric locus. An additional copy of *NPT1* was introduced into PSY316AT, which has an *ADE2* marker inserted in the subtelomeric region of chromosome V (53). As shown in Fig. 3D, additional copies of *NPT1* increased telomeric silencing in an *SIR2*-dependent manner.

Instability of the rDNA has been shown to be a major cause of yeast replicative aging. To test whether *NPT1* extends life span by increasing stability at this locus, we determined the rate of rDNA recombination in 2x*NPT1* and 2x*SIR2* strains. This was achieved by measuring the rate of loss of an *ADE2* marker inserted at the rDNA. As shown in Fig. 3E, an additional copy of *NPT1* decreased rDNA recombination by 2-fold, similar to the 2x*SIR2* and 2x*NPT1* 2x*SIR2* strains. When *sir2* was deleted from the 2x*NPT1* strain, rDNA recombination increased dramatically to the levels of a *sir2* null strain (Fig. 3F). These results are consistent with a model in which *NPT1* extends replicative life span by increasing the ability of Sir2 to inhibit rDNA recombination.

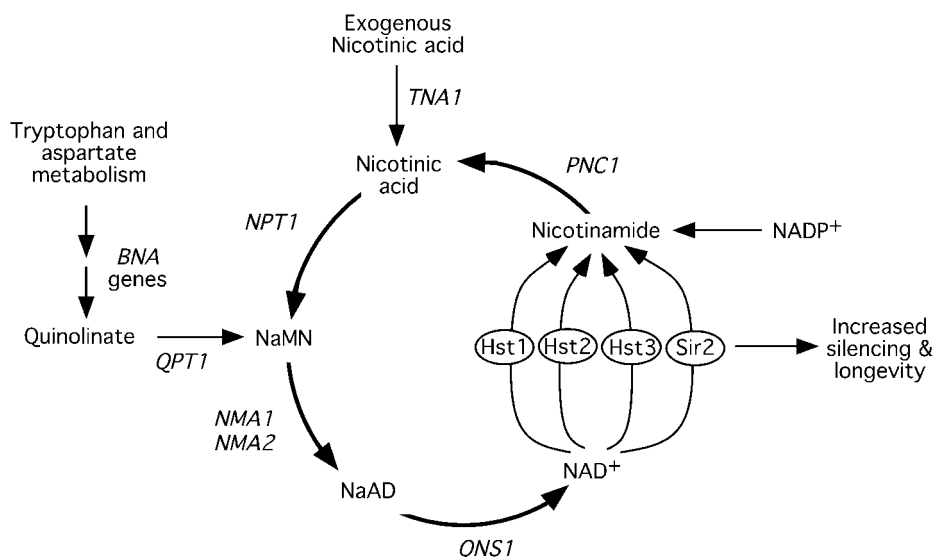
One plausible explanation for the increase in rDNA silencing associated with additional copies of *NPT1* is that the telomeric Sir2 in these strains is relocalized to the rDNA, which would result in the loss of telomeric silencing. We have shown that additional copies of *NPT1* increase telomeric silencing in a *SIR2*-dependent manner, arguing against relocalization of Sir2 from telomeres as the mechanism of life span extension. Another possible explanation is that additional *NPT1* up-regulates Sir2 expression. By Western blotting we found that the steady-state levels of Sir2 did not change in response to additional *NPT1* (data not shown). A third possibility for the increase in rDNA silencing is that additional *NPT1* stimulates overall Sir2 activity. Although it is not currently possible to measure this activity *in vivo*, this idea is consistent with our findings that additional *NPT1* enhances each of the *SIR2*-dependent processes thus far examined.

Caloric Restriction Does Not Alter *NPT1* Expression or Localization—Given that additional *NPT1* and caloric restriction appear to extend life span via the same pathway, we tested whether caloric restriction acts by increasing *NPT1* expression. A triple hemagglutinin epitope (3xHA) tag was added to the carboxyl terminus of Npt1 by integrating a 3xHA-kanamycin resistance cassette into the native *NPT1* locus. We confirmed that the fusion protein was functional by assaying its ability to maintain wild type levels of rDNA silencing (data not shown). *NPT1* levels were then determined in strains grown on (0.5%) glucose medium and in the long-lived *cdc25-10* strain, which is considered a genetic mimic of caloric restriction (19). As shown in Fig. 4 (A and B), no increase in *NPT1* expression was detected at the mRNA or protein level. In fact under low glucose conditions a consistent ~2-fold decrease in *NPT1* expression was observed. We did not detect significant changes in *NPT1* expression after heat shock or exposure to MMS or paraquat (Fig. 4, C and D). We conclude that caloric restriction does not increase longevity by up-regulating *NPT1* expression.

Given that *NPT1* expression was not enhanced in response to

FIG. 6. Model for life span extension via increased flux through the NAD⁺ salvage pathway.

Type III histone deacetylases such as Sir2 and Hst1–4 catalyze a key step in the salvage pathway by converting NAD⁺ to nicotinamide. Additional copies of *PNC1*, *NPT1*, *NMA1*, and *NMA2* increase flux through the NAD⁺ salvage pathway, which stimulates Sir2 activity and increases life span. Additional copies of *QNS1* fail to increase silencing. Unlike other steps in the pathway, its substrate cannot be supplied from a source outside the salvage pathway and is therefore limiting for the reaction. Abbreviations: NAD⁺, nicotinamide adenine dinucleotide; NaMN, nicotinic acid mononucleotide; NaAD, desamido-NAD⁺.



caloric restriction, we examined the possibility that the activity of this protein may be modulated by other means. Specifically, we examined the subcellular localization of GFP-tagged Npt1 in live cells grown in complete or low glucose medium. To our surprise, Npt1 was observed throughout the cell with an apparent concentration of the protein in the nucleus of most cells (Fig. 4E). The large regions of exclusion correspond to vacuoles. These findings raise the intriguing possibility that a significant fraction of NAD⁺ is regenerated in the nucleus. In low glucose medium the localization pattern of Npt1-GFP was unaltered, indicating that there is no gross relocalization of Npt1 in response to caloric restriction (data not shown).

If our hypothesis is correct that the entire NAD⁺ salvage pathway exists in the nuclear compartment, then we should expect that other enzymes in the pathway will show a similar localization pattern to Npt1. Based on the bacterial salvage pathway, the step immediately downstream of *NPT1* is predicted to be catalyzed by a nicotinate mononucleotide adenylyltransferase (NaMAT). There are two yeast ORFs with similar homology to NaMATs from other species, *YLR0328* and *YGR010*, which we have designated *NMA1* and *NMA2*, respectively. To localize these two proteins, a GFP cassette was integrated in-frame prior to the stop codon of each ORF to generate carboxyl-terminal fusions. As shown in Fig. 4F, Nma2-GFP was concentrated in the nucleus in the majority of cells, in a pattern identical to that of Npt1-GFP. This finding further supports our hypothesis that NAD⁺ is recycled from nicotinamide entirely within the nucleus. The localization pattern of Nma1 could not be determined due to low expression levels (data not shown).

Identification of Other Putative Longevity Genes in the NAD⁺ Salvage Pathway—The discovery that Nma2 shows a similar localization to Npt1 prompted us to test whether other genes in the NAD⁺ salvage pathway could have similar effects to Npt1 when overexpressed. Although the bacterial genes in NAD⁺ salvage pathway have been studied in detail, in *S. cerevisiae* some of the key genes in the pathway remain to be characterized. *PNC1*, a recently identified gene, encodes a nicotinamidase, which catalyzes the conversion of nicotinamide to nicotinic acid, the step immediately upstream of *NPT1*. As discussed above, the two genes *NMA1* and *NMA2* encode NaMNATs, which catalyze the step immediately downstream of *NPT1*. In bacteria, the next step in the pathway, the generation of NAD⁺, is catalyzed by an NAD synthetase. An uncharacterized ORF, *QNS1/YHR074*, shows high homology to NAD synthetases.

Each of these salvage pathway genes was integrated as a

single copy into the *URA3* locus of W303AR5 and PSY316AT and assayed for silencing as previously described. Additional copies of either *PNC1*, *NMA1*, or *NMA2* increased rDNA and telomeric silencing to levels similar to those in a 2x*NPT1* strain (Fig. 5, B and C). In contrast, additional copies of *QNS1* had no effect on either rDNA silencing (Fig. 5B) or telomeric silencing (data not shown). As discussed below, these results indicate there are multiple steps that can affect the rate of the pathway and that the two homologs *NMA1* and *NMA2* may have overlapping functions.

DISCUSSION

NPT1 encodes a key component of the yeast salvage pathway that recycles NAD⁺, a cofactor of Sir2. We have shown that additional copies of *NPT1* increase life span by up to 60% in a *SIR2*-dependent manner. It has been proposed that longevity in yeast may be associated with increased NAD⁺ levels. However, we have shown that in strains with additional copies of *NPT1*, steady-state NAD⁺ levels are unaltered. Furthermore, the NAD⁺/NADH ratios are also similar to wild type cells, indicating that total cellular redox state is not dramatically altered either.

We have also shown that *sir2* mutants have wild type NAD⁺ levels, implying that Sir2 is not a major consumer of NAD⁺. Nevertheless, by virtue of its ability to convert NAD⁺ to nicotinamide, Sir2 should be responsive to increased flux through the salvage pathway (Fig. 6). Thus, although steady-state levels of NAD⁺ remain constant, the turnover of this molecule may be elevated. Localization of GFP-tagged enzymes indicated that at least two of the enzymes in the NAD⁺ salvage pathway are concentrated in the nucleus. Consistent with this, Nma1 and Nma2 have been shown by high throughput two-hybrid screening to interact with Srp1, a protein that acts as a receptor for nuclear localization sequences (54). The same two-hybrid screen also found that Nma1 and Nma2 can interact with themselves and with each other. Perhaps Nma proteins exist as dimers, as is the case for the *Bacillus subtilis* NaMNAT (55), or as hexamers, as is the case for *Methanococcus jannaschii* (56) and *Methanobacterium thermoautotrophicum* NaMNATs (57). It is worth noting that strains disrupted for either *NMA1* or *NMA2* are viable, arguing that they may be functionally redundant, given that the conversion of NaMN to NAD⁺ is apparently essential for viability (58).

In vertebrates, NaMNAT/NMNAT activity is primarily observed in the nuclear fraction of liver cell extracts (59), suggesting that nuclear compartmentalization of the pathway may

be a universal property of eukaryotic cells. Having the salvage pathway in proximity to chromatin may allow NAD⁺ to be rapidly regenerated for silencing proteins. Alternatively, it may permit the coordination of a variety of nuclear activities via the alteration of nuclear NAD⁺ pools. Testing of these hypotheses will not be a simple task but one that will be greatly assisted by the development of a molecular probe for intracellular NAD⁺.

In yeast and many metazoans, a number of long-lived mutants display increased stress resistance. However, there are many examples of mutations that extend life span but provide little protection against stress, indicating that this relationship is not straightforward (4). For example, in yeast the life span extension provided by a *cdc25-10* mutation is not accompanied by heat-shock resistance (19). We have shown that additional copies of *NPT1* or *SIR2* extend life span but do not provide protection against MMS, paraquat, or starvation. Thus, in *S. cerevisiae*, longevity is not linked to a general increase in stress resistance. The only stress-related phenotype that correlated with longevity was heat-shock resistance. Based on genome-wide analyses of gene expression in *sir2Δ* strains, it has been proposed that Sir2 regulates genes other than those at the three silent loci (60), although this interpretation is debated (61). If the interpretation is correct, then it is plausible that the heat-shock resistance we observed in *2xNPT1* and *2xSIR2* strains results from Sir2-mediated silencing of genes that suppress heat-shock resistance.

In bacteria, the Npt1 homolog PncB catalyzes a rate-limiting step in the NAD⁺ salvage pathway (35, 37, 38). In this study we show that additional copies of *PNC1*, *NPT1*, *NMA1*, or *NMA2* all increase rDNA and telomeric silencing. The implication is that, in yeast, multiple steps can affect the rate of the pathway. Such a proposal is consistent with Metabolic Control Analysis, a theory based on the observation that flux through most metabolic pathways is controlled by multiple enzymes, rather than by a single rate-limiting step (62). Of all the genes in the salvage pathway, only *QNS1* had no effect on silencing, suggesting that it is the only enzyme in the pathway limited by substrate availability. This is likely due to the fact that the predicted substrate for Qns1, desamido-NAD⁺, is the only intermediate that cannot be supplied from a source outside the salvage pathway (see Fig. 6).

In yeast and metazoans there are multiple members of the Sir2 family, many of which have been shown (or are predicted) to be NAD⁺-dependent deacetylases (24, 63). This finding, combined with the fact that some Sir2 family members are cytoplasmic (64, 65), suggests that reversible acetylation may be a much more prevalent regulatory mechanism than previously thought (66). This would place the NAD⁺ salvage pathway in a pivotal position, coordinating the activity of this group of effector proteins in response to cellular energy status.

It is now widely accepted that there are conserved pathways for the regulation of longevity (4, 5). The extent of this conservation is exemplified by the discovery that additional copies of *C. elegans sir-2.1* also extend life span in that organism (31). Our findings show that several *SIR2*-dependent processes can be enhanced by manipulation of the NAD⁺ salvage pathway in yeast, and this may hold true for higher organisms. We have identified *NPT1* homologs in every genome we have examined, and all possess a highly conserved region around a histidine residue that, in *Salmonella*, greatly stimulates catalysis when phosphorylated (67). This mode of regulation may permit the design of mutations or small molecules that increase Npt1 activity. Together, our findings show that Npt1 and other members of the salvage pathway are attractive targets for small

molecules that may mimic the beneficial effects of caloric restriction.

Acknowledgments—We thank D. Moazed, J. Smith, C. Grubmeyer, M. Bryk, F. Winston, A. Andalis, and G. Fink for reagents and advice. We also thank S. Luikenhuis for help with manuscript preparation.

REFERENCES

- Masoro, E. J. (2000) *Exp. Gerontol.* **35**, 299–305
- Vanfleteren, J. R., and Braeckman, B. P. (1999) *Neurobiol. Aging* **20**, 487–502
- Zainal, T. A., Oberley, T. D., Allison, D. B., Szweida, L. I., and Weindruch, R. (2000) *FASEB J.* **14**, 1825–1836
- Kenyon, C. (2001) *Cell* **105**, 165–168
- Guarente, L., and Kenyon, C. (2000) *Nature* **408**, 255–262
- Kirkwood, T. B., and Rose, M. R. (1991) *Philos. Trans. R. Soc. Lond. B Biol. Sci.* **332**, 15–24
- Barton, A. (1950) *J. Gen. Microbiol.* **4**, 84–86
- Sinclair, D. A., Mills, K., and Guarente, L. (1997) *Science* **277**, 1313–1316
- Mortimer, R. K., and Johnston, J. R. (1959) *Nature* **183**, 1751–1752
- Kennedy, B. K., Austriaco, N. R., Jr., and Guarente, L. (1994) *J. Cell Biol.* **127**, 1985–1993
- Kim, S., Villeponteau, B., and Jazwinski, S. M. (1996) *Biochem. Biophys. Res. Commun.* **219**, 370–376
- Ashrafi, K., Lin, S. S., Manchester, J. K., and Gordon, J. I. (2000) *Genes Dev.* **14**, 1872–1875
- Lin, S. S., Manchester, J. K., and Gordon, J. I. (2001) *J. Biol. Chem.* **276**, 36000–36007
- Longo, V. D. (1999) *Neurobiol. Aging* **20**, 479–486
- Jazwinski, S. M. (2001) *Mech. Ageing Dev.* **122**, 865–882
- Sinclair, D. A., and Guarente, L. (1997) *Cell* **91**, 1033–1042
- Kaerberlein, M., McVey, M., and Guarente, L. (1999) *Genes Dev.* **13**, 2570–2580
- Park, P. U., Defossez, P. A., and Guarente, L. (1999) *Mol. Cell. Biol.* **19**, 3848–3856
- Lin, S. J., Defossez, P. A., and Guarente, L. (2000) *Science* **289**, 2126–2128
- Defossez, P. A., Prusty, R., Kaerberlein, M., Lin, S. J., Ferrigno, P., Silver, P. A., Keil, R. L., and Guarente, L. (1999) *Mol. Cell* **3**, 447–455
- Tanner, K. G., Landry, J., Sternglanz, R., and Denu, J. M. (2000) *Proc. Natl. Acad. Sci. U. S. A.* **97**, 14178–14182
- Imai, S., Armstrong, C. M., Kaerberlein, M., and Guarente, L. (2000) *Nature* **403**, 795–800
- Smith, J. S., Brachmann, C. B., Celic, I., Kenna, M. A., Muhammad, S., Starai, V. J., Avalos, J. L., Escalante-Semerena, J. C., Grubmeyer, C., Wolberger, C., and Boeke, J. D. (2000) *Proc. Natl. Acad. Sci. U. S. A.* **97**, 6658–6663
- Landry, J., Sutton, A., Tafrov, S. T., Heller, R. C., Stebbins, J., Pillus, L., and Sternglanz, R. (2000) *Proc. Natl. Acad. Sci. U. S. A.* **97**, 5807–5811
- Laurenson, P., and Rine, J. (1992) *Microbiol. Rev.* **56**, 543–560
- Straight, A. F., Shou, W., Dowd, G. J., Turck, C. W., Deshaies, R. J., Johnson, A. D., and Moazed, D. (1999) *Cell* **97**, 245–256
- Shou, W., Seol, J. H., Shevchenko, A., Baskerville, C., Moazed, D., Chen, Z. W., Jang, J., Charbonneau, H., and Deshaies, R. J. (1999) *Cell* **97**, 233–244
- Shou, W., Sakamoto, K. M., Keener, J., Morimoto, K. W., Traverso, E. E., Azzam, R., Hoppe, G. J., Feldman, R. M. R., DeModena, J., Moazed, D., Charbonneau, H., Nomura, M., and Deshaies, R. J. (2001) *Mol. Cell.* **8**, 45–55
- Tanny, J. C., and Moazed, D. (2001) *Proc. Natl. Acad. Sci. U. S. A.* **98**, 415–420
- Smith, J. S., Caputo, E., and Boeke, J. D. (1999) *Mol. Cell. Biol.* **19**, 3184–3197
- Tissenbaum, H. A., and Guarente, L. (2001) *Nature* **410**, 227–230
- Jiang, J. C., Jaruga, E., Repnevskaya, M. V., and Jazwinski, S. M. (2000) *FASEB J.* **14**, 2135–2137
- Foster, J. W., Kinney, D. M., and Moat, A. G. (1979) *J. Bacteriol.* **137**, 1165–1175
- Ghislain, M., Talla, E., and Francois, J. M. (2002) *Yeast* **19**, 215–224
- Wubbolts, M. G., Terpstra, P., van Beilen, J. B., Kingma, J., Meesters, H. A., and Witholt, B. (1990) *J. Biol. Chem.* **265**, 17665–17672
- Vinitzky, A., Teng, H., and Grubmeyer, C. T. (1991) *J. Bacteriol.* **173**, 536–540
- Imsande, J. (1964) *Biochim. Biophys. Acta* **85**, 255–273
- Grubmeyer, C. T., Gross, J. W., and Rajavel, M. (1999) *Methods Enzymol.* **308**, 28–48
- Emanuelli, M., Carnevali, F., Lorenzi, M., Raffaelli, N., Amici, A., Ruggieri, S., and Magni, G. (1999) *FEBS Lett.* **455**, 13–17
- Hughes, K. T., Olivera, B. M., and Roth, J. R. (1988) *J. Bacteriol.* **170**, 2113–2120
- Mills, K. D., Sinclair, D. A., and Guarente, L. (1999) *Cell* **97**, 609–620
- Smith, J. S., and Boeke, J. D. (1997) *Genes Dev.* **11**, 241–254
- Lalo, D., Carles, C., Sentenac, A., and Thuriaux, P. (1993) *Proc. Natl. Acad. Sci. U. S. A.* **90**, 5524–5528
- Becker, D. M., Fikes, J. D., and Guarente, L. (1991) *Proc. Natl. Acad. Sci. U. S. A.* **88**, 1968–1972
- Sikorski, R. S., and Hieter, P. (1989) *Genetics* **122**, 19–27
- Guldener, U., Heck, S., Fielder, T., Beinhauer, J., and Hegemann, J. H. (1996) *Nucleic Acids Res.* **24**, 2519–2524
- De Antoni, A., and Gallwitz, D. (2000) *Gene* **246**, 179–185
- Longtine, M. S., McKenzie, A., 3rd, Demarini, D. J., Shah, N. G., Wach, A., Brachat, A., Philippsen, P., and Pringle, J. R. (1998) *Yeast* **14**, 953–961
- Keil, R. L., and McWilliams, A. D. (1993) *Genetics* **135**, 711–718
- Ashrafi, K., Lin, S. S., Manchester, J. K., and Gordon, J. I. (2000) *Genes Dev.* **14**, 1872–1885
- Clancy, D. J., Gems, D., Harshman, L. G., Oldham, S., Stocker, H., Hafen, E., Leivers, S. J., and Partridge, L. (2001) *Science* **292**, 104–106
- Kennedy, B. K., and Guarente, L. (1996) *Trends Genet.* **12**, 355–359
- Gottschling, D. E., Aparicio, O. M., Billington, B. L., and Zakian, V. A. (1990) *Cell* **63**, 751–762

54. Uetz, P., Giot, L., Cagney, G., Mansfield, T. A., Judson, R. S., Knight, J. R., Lockshon, D., Narayan, V., Srinivasan, M., Pochart, P., Qureshi-Emili, A., Li, Y., Godwin, B., Conover, D., Kalbfleisch, T., Vijayadamar, G., Yang, M., Johnston, M., Fields, S., and Rothberg, J. M. (2000) *Nature* **403**, 623–627
55. Olland, A. M., Underwood, K. W., Czerwinski, R. M., Lo, M. C., Aulabaugh, A., Bard, J., Stahl, M. L., Somers, W. S., Sullivan, F. X., and Chopra, R. (2002) *J. Biol. Chem.* **277**, 3698–3707
56. D'Angelo, I., Raffaelli, N., Dabusti, V., Lorenzi, T., Magni, G., and Rizzi, M. (2000) *Structure Fold Des.* **8**, 993–1004
57. Saridakis, V., Christendat, D., Kimber, M. S., Dharamsi, A., Edwards, A. M., and Pai, E. F. (2001) *J. Biol. Chem.* **276**, 7225–7232
58. Winzler, E. A., Shoemaker, D. D., Astromoff, A., Liang, H., Anderson, K., Andre, B., Bangham, R., Benito, R., Boeke, J. D., Bussey, H., Chu, A. M., Connelly, C., Davis, K., Dietrich, F., Dow, S. W., El Bakkoury, M., Foury, F., Friend, S. H., Gentalen, E., Giaever, G., Hegemann, J. H., Jones, T., Laub, M., Liao, H., and Davis, R. W., *et al.* (1999) *Science* **285**, 901–906
59. Hogeboom, G., and Schneider, W. (1950) *J. Biol. Chem.* **197**, 611–620
60. Bernstein, B. E., Tong, J. K., and Schreiber, S. L. (2000) *Proc. Natl. Acad. Sci. U. S. A.* **97**, 13708–13713
61. Bedalov, A., Gatabonton, T., Irvine, W. P., Gottschling, D. E., and Simon, J. A. (2001) *Proc. Natl. Acad. Sci. U. S. A.* **98**, 15113–15118
62. Fell, D. (1997) *Understanding the Control of Metabolism. Frontiers in Metabolism* (Snell, K., ed) pp. 18–25, Portland Press, London
63. Landry, J., Slama, J. T., and Sternglanz, R. (2000) *Biochem. Biophys. Res. Commun.* **278**, 685–690
64. Perrod, S., Cockell, M. M., Laroche, T., Renauld, H., Ducrest, A. L., Bonnard, C., and Gasser, S. M. (2001) *EMBO J.* **20**, 197–209
65. Afshar, G., and Murnane, J. P. (1999) *Gene* **234**, 161–168
66. Shore, D. (2000) *Proc. Natl. Acad. Sci. U. S. A.* **97**, 14030–14032
67. Rajavel, M., Lalo, D., Gross, J. W., and Grubmeyer, C. (1998) *Biochemistry* **37**, 4181–4188
68. Campisi, J. (2000) *Science* **289**, 2062–2063
69. Guarente, L. (2000) *Genes Dev.* **14**, 1021–1026

Manipulation of a Nuclear NAD⁺ Salvage Pathway Delays Aging without Altering Steady-state NAD⁺ Levels

Rozalyn M. Anderson, Kevin J. Bitterman, Jason G. Wood, Oliver Medvedik, Haim Cohen, Stephen S. Lin, Jill K. Manchester, Jeffrey I. Gordon and David A. Sinclair

J. Biol. Chem. 2002, 277:18881-18890.

doi: 10.1074/jbc.M111773200 originally published online March 7, 2002

Access the most updated version of this article at doi: [10.1074/jbc.M111773200](https://doi.org/10.1074/jbc.M111773200)

Alerts:

- [When this article is cited](#)
- [When a correction for this article is posted](#)

[Click here](#) to choose from all of JBC's e-mail alerts

This article cites 68 references, 33 of which can be accessed free at <http://www.jbc.org/content/277/21/18881.full.html#ref-list-1>

VOLUME 277 (2002) PAGES 18881–18890

DOI 10.1074/jbc.A113.111773

Manipulation of a nuclear NAD⁺ salvage pathway delays aging without altering steady-state NAD⁺ levels.

Rozalyn M. Anderson, Kevin J. Bitterman, Jason G. Wood, Oliver Medvedik, Haim Cohen, Stephen S. Lin, Jill K. Manchester, Jeffrey I. Gordon, and David A. Sinclair

PAGE 18883:

During preparation of the manuscript, the same images of yeast colonies were inadvertently shown for two different wild type controls in Fig. 2A. The panel is for visual purposes only. The quantification of three independent experiments is shown in Fig. 2B. The error does not affect the results or conclusions of the study.

Authors are urged to introduce these corrections into any reprints they distribute. Secondary (abstract) services are urged to carry notice of these corrections as prominently as they carried the original abstracts.